

See discussions, stats, and author profiles for this publication at: <https://www.researchgate.net/publication/262600692>

Physico-mechanical properties of bauxite residue-clay bricks

Article in *Journal of Engineering and Applied Sciences* · December 2012

CITATIONS

4

READS

179

5 authors, including:



Ebenezer Annan

University of Ghana

21 PUBLICATIONS 47 CITATIONS

SEE PROFILE



Benjamin Agyei-Tuffour

Rutgers, The State University of New Jersey

35 PUBLICATIONS 60 CITATIONS

SEE PROFILE



Lucas Damoah

33 PUBLICATIONS 156 CITATIONS

SEE PROFILE



David Konadu

University of Ghana

8 PUBLICATIONS 56 CITATIONS

SEE PROFILE

Some of the authors of this publication are also working on these related projects:



Energy View project



Statistical Analysis of Strength and Fracture toughness of Electro-porcelians View project



PHYSICO-MECHANICAL PROPERTIES OF BAUXITE RESIDUE-CLAY BRICKS

Ebenezer Annan¹, Benjamin Agyei-Tuffour¹, Lucas N. W. Damoah^{1,2}, David S. Konadu¹ and Bismark Mensah¹

¹Department of Materials Science and Engineering, University of Ghana, Private Mail Bag, Legon-Accra, Ghana

²Department of Materials Science and Engineering, Missouri University of Science and Technology, 249 McNutt Hall, Rolla, MO, USA

E-Mail: eannan@ug.edu.gh

ABSTRACT

This study is focused on consolidating knowledge on the application of Bauxite residue in the building industry. X-Ray fluorescence (XRF) reports of the bauxite and bauxite residue are given. Physico-mechanical properties of red mud (RM)-Clay (AC) bricks are also presented. The RM-AC bricks have compositions; 90%-10%, 80%-20%, 70%-30%, 60%-40%, 50%-50%, 40%-60% prepared and fired at sintering temperatures 800°C, 900°C and 1100°C. The experimental results obtained showed that at each of the three stated sintering temperatures, bulk density increases as apparent porosity and water of absorption reduces. Bulk densities computed were within the range (1.3-1.8)g/cm³ at 1100°C sintering temperature. Maximum flexural strength was found to be associated with 50%-50% (Red mud-clay) composition at 1100°C. And the compressive strength (3.2-12.5) MPa range found for all batches at 1100°C sintering temperature. Generally, flexural and compressive strengths were increased with higher sintering temperature. The results obtained for various characterization analysis compares well with literature and hold potential in bauxite residue eco-friendly application as fired brick.

Keywords: red mud - clay bricks, bauxite residue, flexural strength, compressive strength.

1. INTRODUCTION

The activities of many industries have yielded by-products that are sometimes not properly handled and may be detrimental to the environment. They are often disposed in nearby dumps, not adhering to environmental regulations. In the building industry, recycling of waste materials is environmentally friendly. One tenable option is their re-use as starting materials for engineering applications.

Red mud (RM) is a solid by-product in the production of alumina by alkaline leaching process of bauxite, generally termed as Bayer Process. It is estimated that approximately 35% - 40% per ton of bauxite treated ends up as waste via Bayer process. Furthermore, about 70 million tonnes of bauxite residue or RM are produced yearly worldwide and are not utilised [1]. Africa has 27% reserves of bauxites deposits and Ghana is known to have one of the high quality bauxites in terms of its turn over in the production of aluminium [2]. The current methods of disposal of the RM in many countries are not safe and hazardous to the ecosystem [3]. The destructive nature of the RM is mainly due to the high alkaline nature having a pH value ranging from 10 to 14 [4]. The seepage of the high pH RM into surface and ground water has damning consequence on potable water supply to humans, livestock and plants [5-7].

Many researchers have enumerated the various applications of RM and some of them are; special cement preparation, iron powder recovery, clay liners stabilizers, aluminium catalytic usage and construction grade brick [4, 8-11]. The most striking application, in our opinion, was its use in the building industry as bricks. In 1986-1995, the building research in Jamaica, conducted a research to mitigate the effect of adverse effects of RM disposal to the environment. They were successful in stabilizing Bayer

RM and consequently produced bricks [12]. It must be noted that their RM brick had cement as a raw material.

At sintering temperatures of 1000-1100°C, Knight *et al.*, [13] reported apparent porosity 40-48%, flexural strength (17.23-27.09) MN/m² and compressive strength of 42-83.9MN/m². They attributed the high strength and fracture toughness (0.39-0.69) MN/m^{3/2} to glassy state phases in the matrix. Perez *et al.*, [14] suggested 1100-1200°C sintering temperatures; attesting better sintering at those temperatures. A 100% bauxite residue ceramic was also sintered at 950 °C by di San Filippo and Usai [15], and achieved compressive strengths comparable to masonry bricks with a shaping pressure of 5000 kg/m² and sintering time greater than 48 hours. Furthermore, Moya *et al.*, [16] reported that sintering of 100% bauxite residue ceramics should take place at 1200°C. Using ASTM C373-88 and ASTM C326-82 standard protocols, at a heating rate of 5°C/min and 1000°C sintering temperature, high sintered body (bulk density 1.7g/cm³) was also produced by Sglavo *et al.*, [17]. Literature [1-17] confirms sintering temperatures from 950°C for ceramic bodies. This produces fired ceramic piece that have high shrinkage and minimum water absorption, and thus ultimately result in greater mechanical strengths.

In this paper, investigations were carried out on the use of RM in brick production using plastic clay as a binder to impart green strength in the forming of the test pieces. Results of physical properties, flexural and compressive strengths of batch formulations red mud-Abonko clay (RM-AC) sintered at 800°C, 950°C, and 1100°C are discussed.



2. MATERIALS AND METHODS

2.1. Preparation of samples and brick fabrication

Bauxite and Abonko clay were mined from Kibi, Eastern region of the Republic of Ghana. The bauxite was reduced to 100 μ m particle size via wet milling using ball-Thomas mill device and granulometer. It was digested with 2M caustic soda at temperature range of 135°C - 150°C in volumetric flask. The homogenous mixture was allowed to cool at ambient temperature and allowed to sediment. The liquid phase was decanted and residue (RM) dried in autoclave at 110°C for 48 hours. The samples were then allowed to cool to room temperature for 24hours (depends on moisture condition). Chemical analysis of the RM was done using X-ray fluorescence equipment (Spectro X-Lab, 2000). Batch formulations of brick formed are given in Table-1. The RM-AC composite batches were prepared in a batch mixer under the same condition. RM- AC bricks with dimensions 6cm x 3cm x 2cm were produced. Batch formulations of brick formed are given in Table-1. For each formulated batch, brick test pieces were fired at temperatures 800°C, 950°C and 1100°C at a heating rate of 5°C/min for 5 hours.

Table-1. Batch formulation of RM-AC bricks.

| Batch sample | Red mud (% Wt) | Abonko clay (% Wt) | CODE |
|---------------|----------------|--------------------|------|
| Test sample A | 90.00 | 10.00 | TSA |
| Test sample B | 80.00 | 20.00 | TSB |
| Test sample C | 70.00 | 30.00 | TSC |
| Test sample D | 60.00 | 40.00 | TSD |
| Test sample E | 50.00 | 50.00 | TSE |
| Test sample F | 40.00 | 60.00 | TSF |



Figure-1. RM-AC briquettes.

2.2. CHARACTERIZATION TECHNIQUES

2.2.1. Chemical characterization

The chemical compositions of the bauxite, RM and AC were determined by using Spectro X-Lab-2000 (XRF equipment). The particles sizes used were \square 100 microns.

2.2.2 Physical characterization

Plasticity Index is the numerical difference between the liquid limit and the plastic limit for a particular material and indicates the magnitude of the range of moisture content over which the soil remains plastic. The Cassagrande device, ELLE international was used for plasticity index (PI) testing. It has a cup and grooving tool and is mechanically operated. Equation (1) below was used in the computations.

$$\text{Plasticity Index,} \quad PI = LL - PL \quad (1)$$

Where, *LL* is liquid limit and *PL*, plastic limit.

The water of absorption value gives a rough measure of the extent to which the product is susceptible to seepage of water through its pores when immersed in water. In this work, the average weight of fired briquette is measured, and that when soaked in water for an hour is also weighed. The relations used in computing water of absorption (*WA*), apparent porosity (*AP*), and bulk density (*BD*) are given in equations (2), (3) and (4), respectively.

$$WA(\%) = \frac{S_w - F_w}{F_w} \times 100 \quad (2)$$

$$AP(\%) = \frac{W_c - W_a}{W_c - W_b} \times 100 \quad (3)$$

$$BD = \frac{W_a}{W_c - W_b} \quad (4)$$

Where *S_w* is soaked weight, *F_w* is fired weight, *W_a* is weight dry sample in air, and *W_b* is weight of soaked sample in water, and *W_c* is weight of soaked sample in air.

ASTM C830-09 and ASTM D6111-09 standard tests were followed to determine the porosity and bulk density respectively. Computed values of bulk density and apparent porosity plotted for various batch formulations. Water of absorption data and apparent porosity variation as the content of AC increases are presented and discussed.

2.2.3. Flexural strength

Using three point bending testing (ASTM C99/C99M-09 standard protocols), the flexural strength of the test bars were determined. Figure-2 represent the test configuration for specimen dimension of (20 x 1 x 1) cm³ and distance 7.6cm (between supports), monotonic loading was done at 1.85kg/min till point of fracture. Equation (5) was used in computing flexural strengths and the average values were recorded from two tests. The effect of clay content the flexural strength values were investigated.



$$\sigma = \frac{3FL}{2hd^2} \quad (5)$$

Where F is load, d is thickness, h is width, and L is distance between supports used.

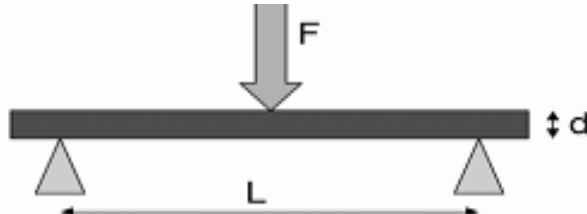


Figure-2. Schematic Three Point Bending Method.

2.2.4. Compressive strength

The ASTM C99/C99M - 09 standards were followed for this analysis using Model CAT C46L2 Compressive device. Two specimen of each batch was subjected to a load between 500 N and 2500 N, at a uniform rate. The two test specimens from each batch formulation had dimensions 1cm x 2cm. The material's response (maximum stress) to the applied load before failure was measured and compressive strength (C.S) obtained using equation (6). The computed compressive strengths of the brick composites were studied.

$$C.S = \frac{P}{BW} \quad (6)$$

Where P , is Average compressive force exerted on samples, B , and W are breadth and width of the rectangular specimen.

3. RESULTS AND DISCUSSIONS

3.1. Chemical analysis

The physico-chemical properties of ceramic materials highly depend on its composition [19]. The results of XRF analysis of the bauxite and RM are presented in Table-2 which agrees with Liu *et al.*, [12]. This data gives an idea of the various percentages of the constituents of bauxite and red mud. The dominance of the red colour in the RM and bauxite is attributed to the fairly

well distributed particles of iron oxide in both samples [1, 20].

Other oxides found with weight percentages less than 1% are for Kibi bauxite: MgO (0.08%), P₂O₅ (0.18%), SO₃ (0.30%), K₂O (0.04%), MnO (0.01%) and for RM: MgO (0.22%), P₂O₅ (0.18%), SO₃ (0.26%), K₂O (0.04%), and MnO (0.01%). Minor elements found in both samples include V, Cr, Co, Ni, Cu, Zn, Ga, As, Y, Ba, Pb and U.

Table-2. Major oxides compositions from XRF analysis.

| Major oxides | Kibi bauxite (%) | Red mud (%) |
|--------------------------------|------------------|-------------|
| Al ₂ O ₃ | 37.42 | 22.08 |
| SiO ₂ | 3.24 | 3.13 |
| Fe ₂ O ₃ | 27.84 | 38.41 |
| Na ₂ O | 2.14 | 5.83 |
| TiO ₂ | 4.97 | 4.56 |
| CaO | 0.04 | 1.05 |
| Loss on ignition (L.O.I) | 23.30% | 24.20% |

The presence of the fluxes such as Na₂O, K₂O, and CaO enhance liquid phase sintering by forming low melting eutectic compounds and also marks beginning of sintering process [21, 22]. They help to reduce the sintering temperature of the brick by melting at a lower temperature and dissolving other grains such as quartz which melt at high temperatures. This may lead to glassy phases which enhance strength and fracture toughness [13].

3.2. PHYSICAL-MECHANICAL PROPERTIES

3.2.1. Plasticity index

The PI for BRM and AC were found to be 6.1 (silt) and 41 (highly plastic), respectively. Figure-3 presents the location of BRM and AC on the Casagrande plasticity chart. Based on the silty nature of the BRM, it can be predicted to shatter when moulded and fired at temperatures above 400°C. This may be due to lack of enough cohesive bonding during dehydration and non-uniform heating cycle.

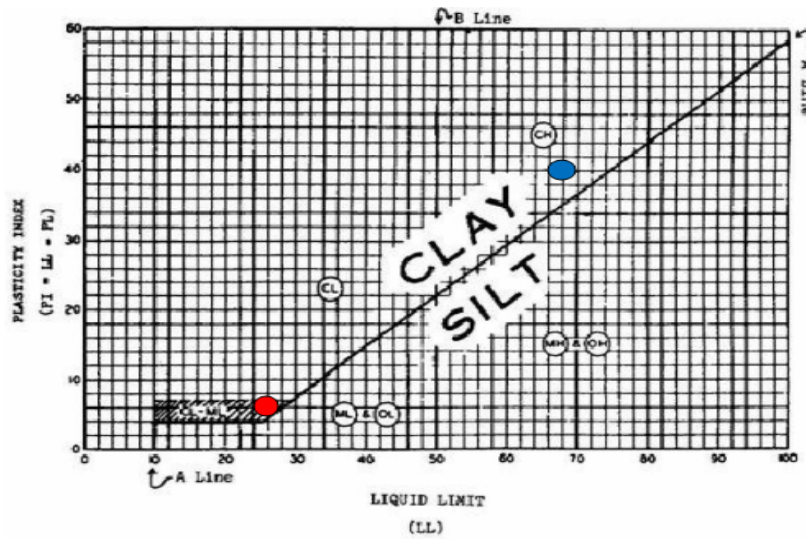


Figure-3. Plot of plasticity index of Abonko clay (blue dot) and red mud (red dot).

3.2.2. Bulk density

Figure-4 shows the plot of the bulk against sintering temperature for the various batches. As the content of clay increases, bulk density values are found to increase for all the sintering temperature. The maximum bulk density of 1.8g/cm^3 was found to be associated with TSE at a sintering temperature of 1100°C . However, TSF

had a lower value than TSE. This may be due to inhomogeneity in the composition. And such observation may result in more potential crack planes of the composite during firing which can affect the mechanical and other properties of the sintered piece. The densification trend for all batches was observed to increase as sintering temperature rises.

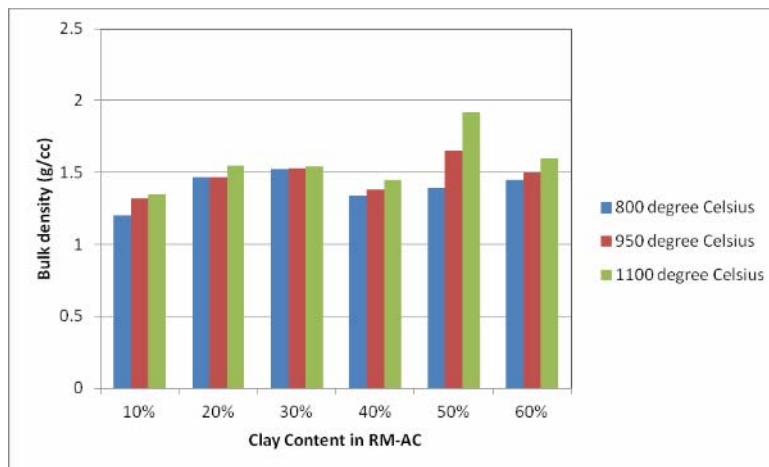


Figure-4. Bulk Density plot at Sintering Temperatures (800°C , 950°C , 1100°C).

Generally for firing ceramic materials, vaporization of water takes place from ambient to 250°C , burning of carbonaceous materials occurs between 250°C to 550°C , while de-hydroxylation of the clay mineral lattice:- expulsion of hydroxyl groups [19, 23] occur for further firing. At this stage the clay losses its plasticity and because there is a breakdown of its mineral lattice and often referred to as "dead clay". If any free quartz exists, there is an inversion of the α - β quartz phases. Above 600°C , sintering commences resulting in the reduction of pores and pore sizes. Densification proceeded very fast, because of the high content of fluxes in the samples. The

fluxes allowed an easy formation of low melting compounds which bonded the particles together. Dense bodies are formed beyond this temperature and at 1000°C ; vitrification of the dense bodies begins. At this temperature, nucleation of primary mullite begins with the evolution of heat [1, 18].

3.2.3. Apparent porosity and water of absorption

With the exception of TSB and TSC, the remaining batch formulations were found to have apparent porosity values decreasing with increasing sintering temperatures. The most sintered piece was TSE with



apparent porosity 50% (at 800°C sintering temperature) and 28% (at sintering temperature 1100°C) whereas the least was TSA with 4% reduction for same specified range of sintering temperatures. Knight *et al.*, [13] reported 40-48% apparent porosity values at a sintering temperature of 1000-1100°C of raw RM having particles \square 75 μ m. Figure-5 compares data of water of absorption and apparent porosity for the various batches at 1100°C. Water of

absorption has inverse relationship with increasing sintering temperatures. It is found to have same relation with apparent porosity, and also inverse with other mechanical properties. This is due to pores reduction as a result of sintering. It is worth knowing that important feature in firing of ceramic materials is in dehydroxylation [18], and reduced crack formation (in proper heating rate) [24].

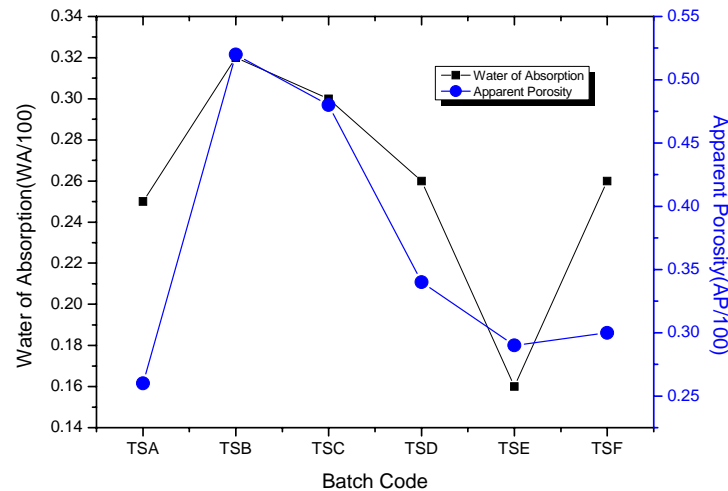


Figure-5. Water of Absorption and Apparent Porosity plot at 1100°C.

3.2.4. Flexural strength

With the increase in temperature, better sintering occurred and there was reduction in average pore size. For same sintering temperatures, flexural strength was observed to increase with increasing composition of AC to TSE and dropped at TSF as shown in Figure-6. It might be as a result of effective cohesion between particles as the binder percentage increases. It has been observed that binder increment minimizes porosity by increasing the

cohesion forces and decreasing their inter-particles separation [23]. This in turn increased their associated bulk densities and resulted in high strength of the green bodies. However, TSF (40%: 60%) strength was less than that of TSE for all temperatures. It is suspected that in the TSF the binder phase becomes the continuous phase, that which bears the greater part of the load. The limit of AC in the composite is set at 50% to obtain optimal properties.

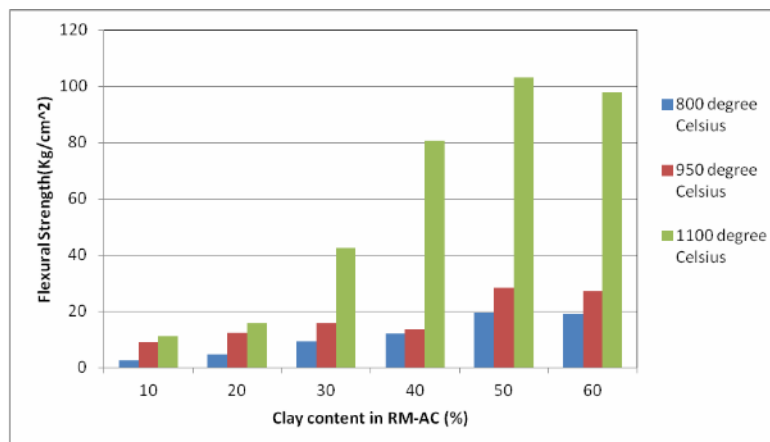


Figure-6. Effect of Clay Content on Flexural Strength.

At 1000°C and above, the presence of fluxes in the test piece begins to yield glassy phase along the grain boundaries of the mixtures. This in turn remarkably

increases the bulk density and consequently flexural strength increase. The net effect is that higher temperature-to-AC concentration would yield high mechanical strength



as demonstrated by the batch TSE at 1100°C. Batches TSE and TSF (103.1kg/cm² and 98 Kg/cm²) could be used in over burden structural components based on India standard specification (100-over 240kg/cm² at 1100°C).

3.2.5. Effect of Clay on Apparent Porosity and Flexural Strength

From Figure-7 it is observed there is an inverse relation between flexural strength and apparent porosity. As the composition of the binder increases for same temperature, apparent porosity is observed to be

decreasing. Manoharan *et al.*, 2011 [18] have reported the densification and reduction of crack formation at higher temperatures with heating rate of 10°C/min. And that as the percentage of porosity increases, flexural strength reduces; that is the mixture has more pores and therefore an applied load to the brick transversely may propagate through the brick easily than compared with low percentage of pores [23]. For flexural strength within tolerable limits of standards, the binder compositions must be between 30% - 60%.

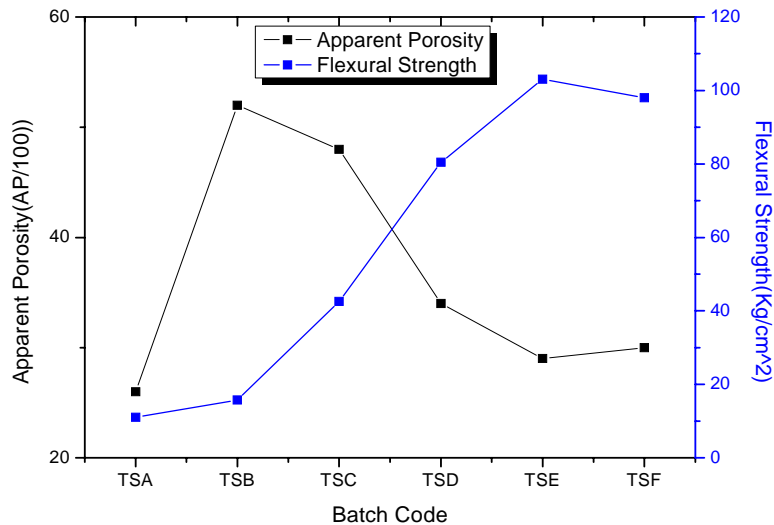


Figure-7. Flexural Strength and Apparent Porosity at 1100°C.

3.2.6. Effect of clay content on water of absorption and bulk density

As the temperature of brick increases, densification occurs. This implies reduction in pore sizes and also percentage of pores; increase in cohesive forces between inter-particles and also intra-particles of the brick

compositions are expected. The absorption of water is mainly through the pores and reduction in pore size apparently corresponds to decrease in water of absorption. This is demonstrated in Figure-8. As the firing temperature rises, ceramic bricks generally undergo de-hydroxylation [18] and therefore bulk density increases.

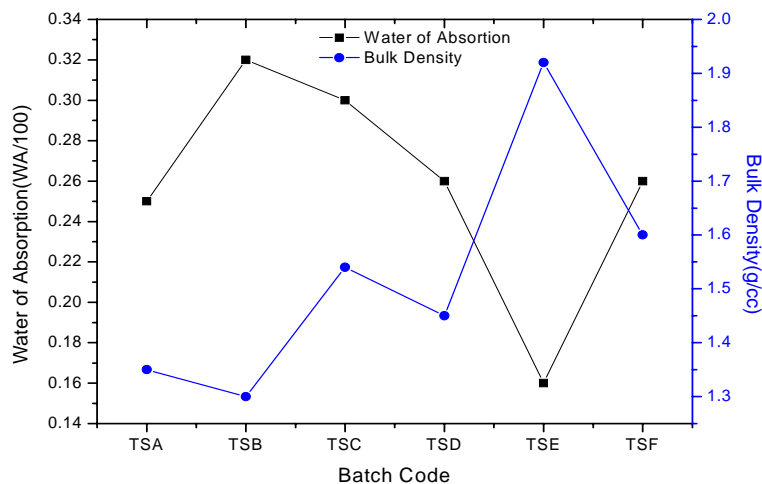


Figure-8. Clay content effect on water of absorption and bulk density at 1100°C.



3.2.7. Compressive strength and porosity

Figure-9 shows the effect of Abonko clay content in the RM-AC brick fired at 1100°C. A comparative plot with the apparent porosity indicates inverse relation. The maximum compressive strength of 12.5MPa for TSE batch

indicates a high homogenous mixture and effective adhesion between the RM and the AC particles. The maximum compressive strength for all batches was found to be generally increasing with increasing firing temperature [24].

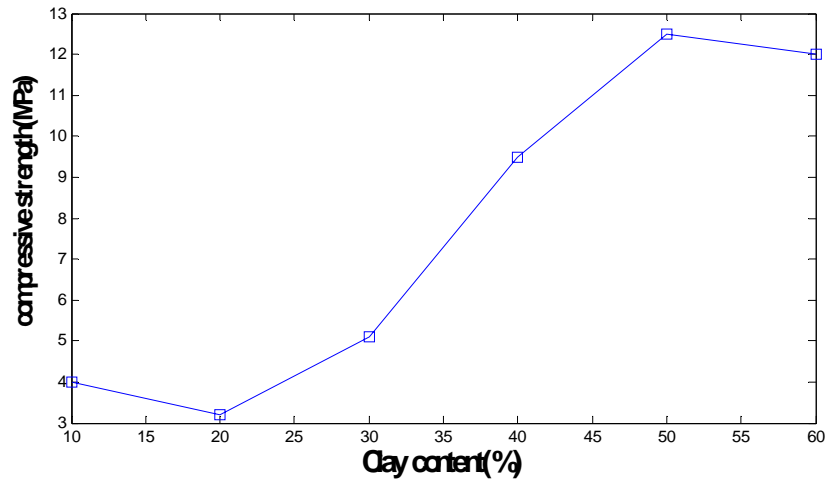


Figure-9. Effect of clay content on Compressive Strength at 1100°C.

However, at 1100°C firing temperature, TSF compressive strength was found to be lower than that of TSE. This may be due to the uneven mix, resulting in more RM particle to particle adhesion, as compared to stronger clay-RM bonds [1, 23, 24]. Additionally, the glassy AC phases become the main load bearer rather than complimenting the load bearing BRM in TSF, which leads to lower strength than TSE. Agglomeration of the clay particles may also contribute to overall strength reduction of mixture [1].

CONCLUSIONS

Feasibility of applying Bayer RM as a raw material in burnt brick production for building applications was investigated. Bricks were made from batch mixes of RM and high plasticity clay material, AC, in varying amounts. The physico-mechanical properties considered for different RM content are apparent porosity, water of absorption, bulk density, flexural and mechanical strengths at firing temperatures of 800°C, 950°C, and 1100°C. The following conclusions can be drawn based on the results obtained from this investigation:

- Sintering at 1100°C produced the brick with the best properties. Apparent porosity and water of absorption reduced while the flexural, compressive strength and the bulk densities increased at higher sintering temperature.
- TSE formulation which contained 50% each of RM- AC brick produced the brick with the best combination for the required application, considering the properties looked into in this research. Optimal properties were recorded for this composition. Other batch formulations were also within tolerable limits (20-30%) and may be employed in lighter weight structural applications.

- High compressive and flexural strength values are due to the uniformity of the composite, strong cohesive forces between both particles of AC and RM resulting from the formation of glassy phase. This is supported by results in the literature [3-21] which employed sintering temperatures within 900°C-1150°C range for better sintering and more durable bricks.

FUTURE WORK

For further understanding, surface morphology and homogeneity studies will be undertaken. Also XRD/EDSA of the RM-AC composites to ascertain their mineralogy and phase transformations during firing will be carried out.

ACKNOWLEDGEMENTS

The authors would like to thank Mr. E.F. Brenya, the Chief Technician at the Department of Materials Science and Engineering, University of Ghana for his immense contribution. We are also grateful to the Scientists of Materials Institute-Centre for Scientific and Industrial Research (CSIR), Ghana, for their technical assistance.

REFERENCES

- [1] Meseaquer S, Pardo F, Jordan M.M, Sanfeliu T and Gonzalez I. 2010. Ceramic behaviour of five Chilean clays which can be used in Manufacture of ceramic tile bodies. *Appl. Clay Sci.* 47: 372-377.
- [2] Kesse G.O. 1985. *The Mineral and Rock Resources of Ghana*. ABalkema. Rotterdam Netherlands.



- [3] John I. Glanville. 1991. Evaluation Report on Bauxite Bricks. IDRC, Ottawa, IDRC FILE, Canada. 3: 86-1039.
- [4] M. Gräfe, G. Power and C. Klauber. 2011. Bauxite residue issues: III. Alkalinity and associated chemistry, Hydrometallurgy. 108: 60-79.
- [5] Pascual J., Corpas F. A., López-Beceiro J., Benítez-Guerrero M. and Artiaga R. 2009. Thermal Characterization of a Spanish Red mud. Journal of Thermal Analysis and Calorimetry. 96(2): 407-412.
- [6] Hind A., Bhargava S. and Grocott S. 1999. The surface chemistry of Bayer process solids: a review. Colloids and Surfaces A: Physicochem. Eng. Aspects. 146: 359-374.
- [7] Nevin Y. and S. Vahdettin. 2000. Utilization of bauxite waste in ceramic glazes. Ceramics International. 26(5): 485-493.
- [8] Cablik V. 2007. Characterization and applications of red mud from Bauxite processing. GOSPODARKA SUROWCAMI MINERALNYMI, tom 23, Zeszyt4.
- [9] Sushil Snigdha and Batra V. S. 2008. Catalytic applications of red mud, an aluminium industry waste: A review. Applied Catalysis B, Environmental. 81: 64-77.
- [10] Kalkam Ekrem. 2006. Utilization of red mud as a stabilization material for the preparation of clay liners. Engineering Geology. 87: 220-229.
- [11] Liu Wancho, Yang Jiakuan and Xiao Bo. 2009. Application of Bayer Red Mud for iron recovery and building material from aluminosilicate residues. Journal of Hazardous Materials. 161: 474-478.
- [12] Karaman S., Ersahin S. and Gunal H. 2006. Firing temperature and firing time influence on mechanical and physical properties of clay bricks. Journal of scientific and industrial research. 65: 153-159.
- [13] J.C. Knight, A.S. Wagh and W.A. Reid. 1986. The mechanical properties of ceramics from bauxite waste. J. Mater. Sci. 21(6): 2179-2184.
- [14] R.G.A. Perez, R. F. Guitian and S. De Aza Pendas. 1999. Industrial obtaining of ceramic materials from the Bayer process red muds. Bol. Soc. Esp. Ceram. 38(3): 220-226.
- [15] P.A. di San Filippo and G. Usai. 1988. The recycling of red mud from the Bayer Process, part 1, production of masonry bricks at a firing temperature of 950 8C, ZI, Ziegelindustrie Int. 41(2-3): 67-74.
- [16] J.S. Moya, F. Morales and V.A. Garcia. 1987. Ceramic use of red mud from alumina plants. Bol. Soc. Esp. Ceram. 26(1): 21-29.
- [17] V.M. Sglavo, R. Camprostrini, S. Maurina, G. Carturan, M. Monagheddu, G. Budroni and G. Cocco. 2000. Bauxite red mud in the ceramic industry. Part 1: thermal behaviour. J. Eur. Ceram. Soc. 20(3): 235-244.
- [18] Manoharan C, Sutharsan P, Dhanapandian S, Venkatachalapathy R and Mohamed Asanulla R. 2011. Analysis of temperature effect on ceramic brick production from alluvial deposits, Tamil Nadu, India Appl. Clay Sci. 54: 20-25.
- [19] Tudisca V., Casieri C., Demma F, Diaz M, Pinol L, Terenzi C. and De Luca F. 2011. Firing technique characterization of black-slipped pottery in Prasnesete by low field 2D NMR relaxometry. Journal Archaeol. Sci. 38: 352-359.
- [20] S. Srikanth, A.K. Ray, A. Bandopadhyay, B. Ravikumar and J. Animesh. 2005. Phase constitution during sintering of red mud and red mud-fly ash mixtures. J. Am. Ceram. Soc. 88(9): 2396-2401.
- [21] Y. Pontikes, C. Rathossi, P. Nikolopoulos, G.N. Angelopoulos, D.D. Jayaseelan and W.E. Lee. 2009. Effect of firing temperature and atmosphere on sintering of ceramics made from bayer process bauxite residue. Ceramics International. 35: 401-407.
- [22] Mackenzie J.KD, Meinhold R. H., Brown I.W.M. and White G.V. 1996. The formation of mullite from Kaolinite under various reactions atmospheres. J. Eur. Ceramics Soc. 16: 115-119.
- [23] Monteiro S.N. and Vieira C.M.F. 2004. Influence of firing temperature on ceramic properties of clays from Campos's dos Goytacazes. Braz. Appl. Clay Sci. 27: 229-234.
- [24] McBurney W.J. 1970. The effect of strength of brick on compressive strength of masonry. Process ASTM Part (II). p. 28.